

Deuterium Gas Charging Experiments with Pd Powders for Excess Heat Evolution

(II) Discussions on Experimental Results and Underlying Physics

A.Takahashi^{1*}, A. Kitamura², T. Nohmi², Y. Sasaki²,

Y. Miyoshi², A. Taniike², R. Seto¹, and Y. Fujita¹

¹Technova Inc. *akito@sutv.zaq.ne.jp

²(Division of Marine Engineering, Graduate School of Maritime Sciences, Kobe University)

Experimental results obtained for Pd/PdO/ZrO₂ nano-composite samples are summarized and the underlying physics is discussed. Arata-Zhang's May 2008 excess heat result was replicated quantitatively. Using Pd/PdO/ZrO₂ powders (produced by Santoku Co., Kobe Japan), we obtained: 1) D-gas charge in the first phase (zero pressure interval) gave 20~90% excess heat than H-gas charge. 2) In the second phase of pressure rise, significant excess heat (about 2 kJ/g-Pd) for D-gas charge was observed, while near zero level excess heat for H-gas charge was observed. We discuss the underlying surface and nano-particle physics in views of the enhanced surface adsorption potential by fractal sub-nano-scale trapping points on nano-Pd particle, the diffusion to inner shallower Bloch potential of regular Pd lattice, and the drastic mesoscopic and isotopic effect of surface and lattice rearrangement of nano-Pd particle by full D(H)-absorption to make deeper D(H) trapping potentials of surface adsorption (about 2 eV for D) and intermediate surface state trapping.

1. Introduction

The aim of this research, the experimental apparatus, experimental procedure and observed results with deuterium and protium gas charging experiments with various nano-fabricated Pd powders are described in our other two papers in this proceedings¹⁾. The Pd/PdO/ZrO₂ nano-composite samples (about 10 nm diameter Pd particles dispersed in about 7 micron size ZrO₂ flakes) produced very interesting performance with deuterium (D) versus protium (H) absorption and exothermic energy generation.

We discuss our results with 100 nm Pd particle powders and Pd-black powder, and compare our results to the Arata-Zhang work²⁾. Our results with nano-Pd/ZrO₂ samples are interesting because specific surface effects in adsorption and following absorption into inner "lattice" sites appears to be taking place, resulting in

anomalously large stoichiometry values ($x > 1$) of PdD_x and deep trapping potential (or released energy). Compared with the 100 nm Pd particle-powders, 10 nm Pd particles dispersed in ZrO₂ are showed drastic mesoscopic effects with isotopic difference.

2. Trend of Heat-Power Evolution

The evolution of heat and gas-pressure can be evaluated for two phases: the first phase and the second phase, as we show in typical data (Fig. 1).

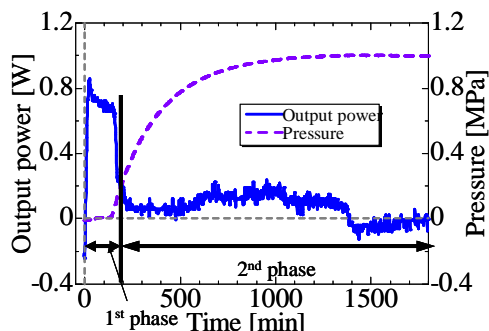


Fig. 1: Typical heat (power) evolution data with Pd/ZrO₂ nano-composite sample with D-gas charge (D-PZ1#1 run)

The first phase is defined as the time-interval where reaction chamber (cell) keeps nominal “zero” gas-pressure. This means almost all D(H)-gas entering the cell is absorbed by the nano-Pd powder. Heat (power) evolution curve in the first phase may be regarded mostly as the normal chemical heat of formation during D(H)-gas absorption into nano-Pd powders. However, there may also be an anomalous nuclear-reaction component to this heat, that we discuss later.

The trend of heat-power evolution in the second phase is very isotope dependent, as shown in typical data in Fig. 2.

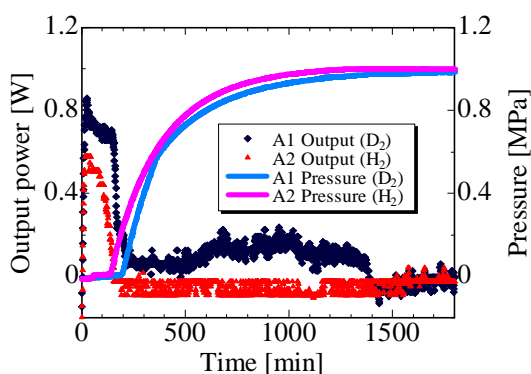


Fig. 2: Typical “excess heat-power” evolution by D-charge for Pd/ZrO₂ sample (D-PZ1#1run), compared with “zero-excess” power level by H-gas charge (H-PZ2#1 run)

The H-gas charge have given “zero” power level (sometimes negative integrated values according to

zero-level drift of calorimetry) in the second phase. Obviously, the D-gas charge to Pd/PdO/ZrO₂ nano-composite sample produced much more heat than the H-gas charge, for both phases.

3. Results and Discussions for First Phase Data

We summarize the integrated data of D(H)/Pd ratios, Heat per one-gram-Pd, Energy per D(H) atom absorption and gas-flow rates in **Table 1** (see end of text).

First we discuss the data for 100 nm Pd-particle powders (D-PP and H-PP runs in Table 1). Loading ratios, D(H)/Pd, are 0.43 and 0.44 respectively for deuterium (D) and protium (H) gas charging. Specific energies per absorbed D (or H) atom E_{1st} (or ΔH_s) values are 0.24 eV/atom-D and 0.20 eV/atom-H. When D(H) is absorbed in metal lattice, surface adsorption traps D(H) molecule (or atom) first and diffuse into inner lattice sites (O-sites of Pd, usually) gradually. Fig. 3 illustrates typical form of surface trapping potential and inner periodical (Bloch) trapping potentials.

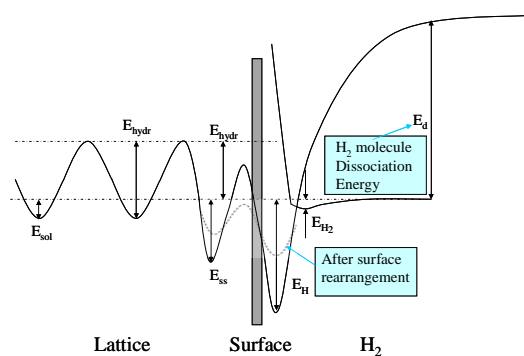


Fig. 3: Image of D(H) trapping potentials at surface adsorption (depth E_H) and lattice absorption (depth E_{Hydr}); trapped D(H) atom diffuses gradually into inner Bloch trapping potentials through the QM tunneling. After full loading ($x=1$ for PdD x), rearrangement of Pd lattice may happen to make shallower potentials.

For known, textbook values³⁾, E_H is about 0.5 eV and

E_{sol} is 0.23 eV. The difference, $E_{\text{H}}-E_{\text{sol}}$, becomes the energy released per D(H)-atom absorption in lattice and is about 0.25 eV for bulk Pd lattice.

The observed $E_{1\text{st}}$ (ΔH_s) values for 100 nm Pd particle powder are near to this value of bulk Pd metal. This means that 100 nm Pd particle works as bulk-metal for D(H) absorption.

We will see $E_{1\text{st}}$ values for Pd-black and Pd/PdO/ZrO₂ nano-composite samples will have given much larger energies (deeper trapping potentials) to show the drastic mesoscopic effects.

Next, we look integrated data for Pd-black samples (D-PB and H-PB runs) in Table 1. $E_{1\text{st}}$ values in averages of runs are 0.70 ± 0.15 eV/atom-D and 0.69 ± 0.10 eV/atom-H. These values are significantly higher than the bulk value about 0.25 eV. For the virgin runs (#1 runs), significantly high loading at PdD_{0.88} or PdH_{0.79} were observed. However, for runs with used samples (#2, #3, #4 runs), loading ratios were as small as 0.23 in average. Nevertheless the specific $E_{1\text{st}}$ values were observed as same as the virgin (#1) runs. This fact means that microscopic active adsorption sites on surface of used Pd-black are working in the same way as the virgin Pd-black sample, although effective area of active surface decreased to 1/3 or less.

We made SEM observation for Pd-black samples of “before” and “after” usage¹⁾. We found the used Pd-black sample powders clumped together to be bigger sizes (about 10 times) than the virgin one and “fractal” nano-structures on surface of virgin Pd-black samples were flattened. We observed excess heat-like event in local time interval of the first phase data for virgin Pd-black and positive excess heat in the second phase, while heat-power level dropped drastically for the used Pd-black runs (#2 run and later runs). We understand that Pd-black has good nano-structure for

making anomalous “CMNS effect”, but the clumping-together effect by absorbing D(H) makes the CMNS effect disable. To overcome this, we need to avoid the clumping-together effect. The clumping-together effect is not sintering, because we did not observe the clumping-together by baking Pd-black powders up to 300 deg C before #1 run.

The idea by Arata-Zhang group²⁾ is of dispersed Pd nano-particles (5 nm diameter) in ceramics as ZrO₂ flakes to block the clumping-together effect.

Now we discuss the integrated data in the first phases for Pd/PdO/ZrO₂ samples (D-PZ and H-PZ runs in Table 1). We observed heat-power levels were strongly dependent on the D(H) gas-flow rate. The larger gas-flow rate has trend to give larger excess heat level in the first phase, but the first phase ends earlier than it does with smaller flow rate. This is understood as the faster gas-flow saturates the D(H) powders more quickly. Therefore, to compare specific values of $E_{1\text{st}}$ (released energy per D(H)-atom), D(H)/Pd (loading ratio) and heat (in kJ) per g-Pd, it is more appropriate to see the underlying physics.

Our first surprise is that for all measured loading ratios, the D(H)/Pd values for the first phases are greater than 1.0. In other words, overloading occurred ($x=1.1$ in average for PdD(H) x stoichiometry) in usual sense, even though the background gas pressure were nearly zero (near vacuum). This must be considered a drastic mesoscopic effect of D(H) absorption by the Pd nano-composite samples. For the known bulk Pd-metal, D(H) atoms are trapped in Bloch potentials (see Fig. 3) at O-sites for $x<1.0$. The observed anomalous data of $x>1.0$ should show that the additional trappings at T-sites happened by the mesoscopic effect (about 5000 Pd atoms existing in a 5 nm diameter particle).

The data for specific released energy $E_{1\text{st}}$ values are

also anomalously large and isotope (D or H)-dependent. These are 2.2-2.5 eV/atom-D and 1.3-2.1 eV/atom-H. Deuterium gives larger E_{1st} values. These released energy values are 5-10 times of the conventional value 0.25 eV for bulk Pd metal. These values are however dependent on the gas-flow rate, and they call for further investigation. As the PZ samples gave drastic mesoscopic effects, compared to the 100 nm Pd powder, we need to do further studies by changing the nano-Pd particle size.

We measured the ratios of [heat/D]/[heat/H] in the first phases. We obtain ratios as 1.94 to 1.3 for the first and second PZ runs. The data we deduced from Arata-Zhang's first phase is about 1.3. We can say our data for the first phase quantitatively replicated the Arata-Zhang result, although Arata-Zhang used 5 nm diameter Pd nano-particles dispersed in ZrO₂ flakes and ours was 10 nm.

4. Excess Heat for the Second Phase

As summarized in Table 1, we observed positive excess heat in the second phase of the D-PZ series runs for virgin (first run) samples. We tested three pairs of samples with simultaneous runs with D-gas in cell A₁ (with the D-PZ5 in cell A₂) and H-gas in A₂ (with H-PZ6 in cell A₁). For the D-PZ5 run, the D-gas cylinder was exhausted in the second phase and the gas pressure decreased (because of a leak), so that excess heat phenomenon was not observed. For the earlier two PZ runs, we observed clear excess heat only for D-gas charging, 2.27 and 2.07 kJ/g-Pd in the time interval of 1600 minutes.

Arata-Zhang gave 29.2 kJ with 24.4 g Pd/ZrO₂ sample. Assuming their sample contained 7.7 g net Pd weight, we get 2.8 kJ/g-Pd for a 3000-minute time interval with higher D-gas pressure (10 MPa maximum), after

correcting specific H-absorption energy E_{1st} value (about 1 eV/atom-H as we observed). We can say that our results for second phase heat was comparable to (or may have exceeded) Arata-Zhang's data, given that their data was for a duration about two times longer, with higher gas pressure.

In Fig. 5, we show the rather steady excess heat evolution for used Pd/PdO/ZrO₂ samples (D-PZ3#2 and H-PZ4#2 runs).

We obtained total excess heat of 3.3 kJ/g-Pd for 9000 minutes of D-gas charging and later evacuation.

Before the end of run, we observed significant excess heat evolution after the evacuation of the A₁ (D-gas) cell. The expanded data is shown in Fig.6.

We speculate that the so called "heat after death event" was observed in the gas-loading experiment. The degassing data after evacuation and baking clearly shows very interesting performance of the Santoku-sample: it retained 100 times more D-atoms after evacuation compared to the Pd-black. (See Fig. 4).

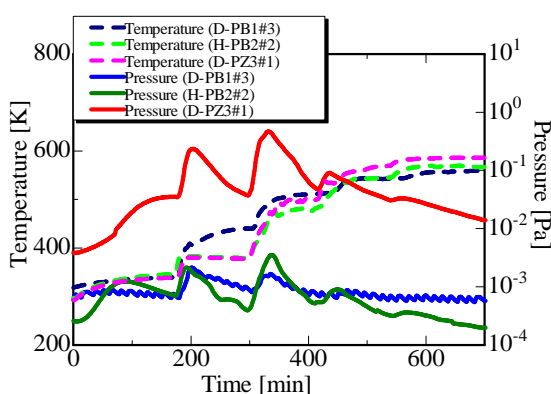


Fig. 4: De-gassing data for Santoku-sample compared with that for Pd-black; Santoku-sample retains 100 times D(H)-atoms by its very deep trapping potentials of the mesoscopic effect of dispersed Pd-nano particles

The heat after death event may take place by trapped

deuteron cluster (namely TSC-formation by Takahashi model⁴⁾) at very deep (maybe about 2 eV for D absorbed PZ-sample) surface adsorption potentials, where deuterons from inner Bloch trapping potentials diffuse gradually to surface trapping points to form transient 4D/TSC cluster and makes $4D \rightarrow {}^4\text{He}+{}^4\text{He}+47.6\text{M eV reactions}^{4)}$ as a green nuclear energy source.

Lastly, we discuss possible chemical energy release by oxidation of charged D(H)-gas, because the samples contained PdO and ZrO₂ components. Figure 4 clearly shows that D(H)-gas was mostly absorbed by Pd in the PZ samples, since Pd-black gave same pattern of degassing.

It is unlikely that the ZrO₂ is making large contributions to these quantities. We have to consider the reduction of PdO_x followed by production of xD₂O (xH₂O) and PdD_y (PdH_y). The reaction energies Q_D and Q_H are evaluated to be $(162.6 \times x + 70.0 \times y)$ kJ and $(156.6 \times x + 58.0 \times y)$ kJ, respectively. For the assumed values of $x = 1 \sim 0$ and $y = 0 \sim 1$, Q_D and Q_H are 0.84 ~ 0.73 eV/D and 0.81 ~ 0.60 eV/H, respectively. These are too small to account for both the observed E_{1st} energies and the isotope effects.

There might be a yet-unknown atomic/electronic process governing the phenomenon in the present mesoscopic system, or the concept of "atom clusters" might apply. However, it seems rather difficult to imagine that such a large isotope effect only occurs in the electronic process of adsorption and/or hydride formation. Some nuclear process as suggested by the 4D/TSC model could be a candidate for the phenomenon.

5. Concluding Remarks

Arata-Zhang's Excess Heat Result was replicated

quantitatively by our more precise heat and loading ratio measurements.

For Pd/PdO/ZrO₂ powders (Santoku-samples):

1) The D-gas charge in the first phase (zero pressure) gave 20-90% excess heat than the H-gas charge.

2) In the second phase, significant excess heat (about 2 kJ/g-Pd) for the D-gas charge, while zero level for the H-gas charge, was observed.

No increase of neutron counts was seen, neither increase of gamma-rays over natural backgrounds.

D(H)/Pd ratios in the end of first phase was $x > 1.0$, namely over-loading ($x = 1.1$ in average). Flow rate dependence of x-values should be investigated further.

Further experiments changing conditions will be fruitful for developing clean energy devices.

Nano-Pd dispersed sample (Santoku, Pd/ZrO₂) retained 100 times more D(H) atoms after evacuation, than the Pd-black case. The mesoscopic effect of Pd-nano-particles, namely surface and lattice rearrangement, probably makes deep D(H) trapping potentials (1.0-2.5 eV). We need to study D(H)-gas flow-rate dependence. Stable excess heat production is expected for #2 and later runs. We need further studies of this. We plan to conduct detection of nuclear products by the B-system.

Replication by other groups is important to confirm our results.

Funding

This is a joint research project of Kobe University and Technova Inc. for fiscal year 2008.

References:

- 1) Y. Sasaki, A. Kitamura, T. Nohmi, Y. Miyoshi, A. Taniike, A. Takahashi, R. Seto, and Y. Fujita; Deuterium Gas Charging Experiments with Pd

- Powders for Excess Heat Evolution, (I) Results of absorption experiments using Pd powders, (this meeting)
- 2) Y. Arata and Y. Zhang: The special report on research project for creation of new energy, J. High Temperature Society, No. 1. 2008.
 - 3) Y. Fukai, K. Tanaka, Y. Uchida: Hydrogen and Metal (in Japanese), Uchida-Roukakuho Pub., Tokyo, ISBN=4-7536-5608-X (2002)
 - 4) A. Takahashi: Cold Fusion 2008- Mechanism of Condensed Cluster Fusion (in Japanese), Kogakusha, ISBN=978-4-7775-1361-1 (2008)

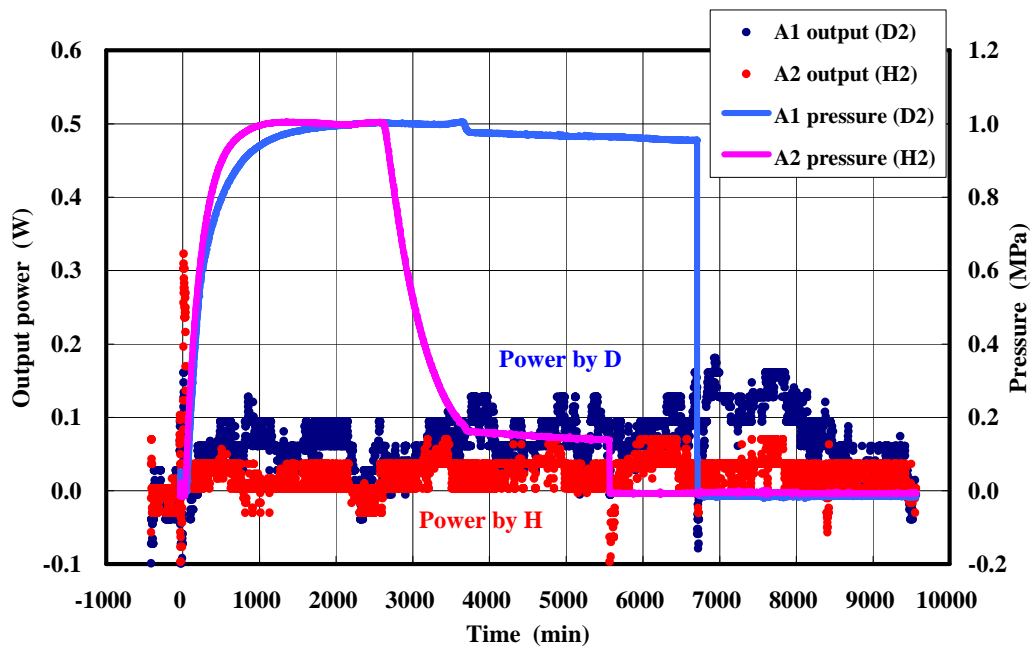


Fig. 5: Long lasting excess heat evolution from a previously used Pd/PdO/ZrO₂ sample

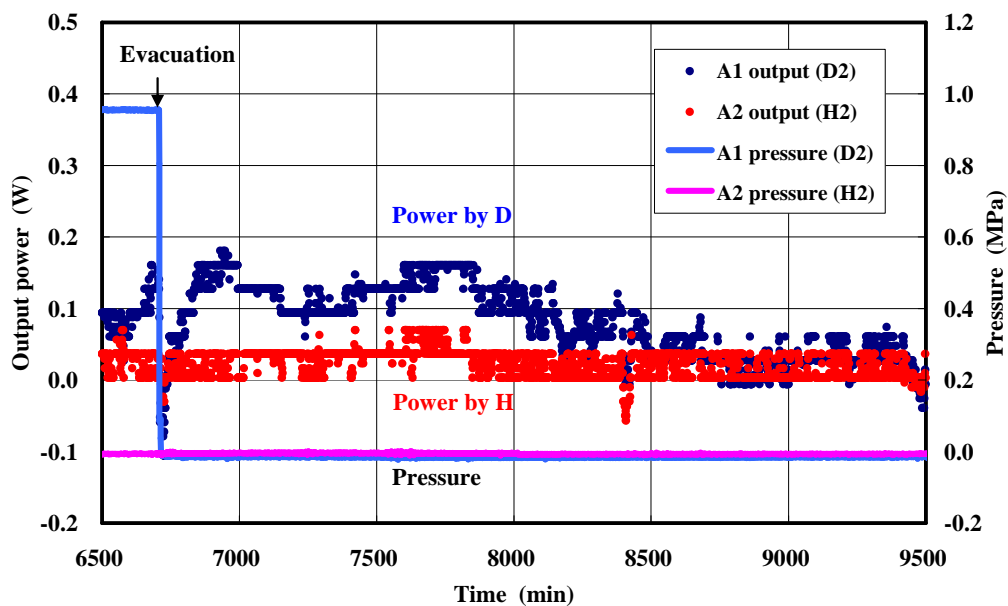


Fig. 6: "Heat after death" event observed after the evacuation of A₁ (D-gas) cell for D-PZ3#2 run

Table 1: Summary of Integrated Data for phase-1 and phase-2, comparing 100 nm Pd powder, Pd-black and Pd/Zr nano-composite samples.

Run number	weight of Pd [g]	Flow rate [sccm]	Output energy [kJ]		Specific output energy [kJ/g]		D/Pd or H/Pd (1 st ph.)	E _{1st} [eV/D(H)]
			1 st phase	2 nd phase	1 st phase	2 nd phase		
D-PP1#1	5.0	2.7	0.5±0.4	2.5±4.1	0.10±0.07	0.52±0.83	0.43	0.26±0.14
D-PP1#2	5.0	3.8	0.5±0.2	4.0±4.4	0.10±0.05	0.79±0.88	0.44	0.25±0.09
H-PP2#1	5.0	5.4	0.4±0.2	2.6±3.9	0.08±0.03	0.53±0.80	0.44	0.20±0.07
D-PB1#1	3.2	3.6	1.7±0.3	8.3±4.5	0.54±0.10	2.60±1.40	0.88	0.67±0.12
H-PB2#1	3.6	4.2	1.6±0.3	(-2.2±4.6)	0.45±0.08	(-0.62±1.30)	0.79	0.62±0.11
D-PB3#1	20.0	2.9	9.3±1.1	1.1±0.5	0.47±0.06	0.06±0.02	0.79	0.65±0.08
D-PB3#2	20.0	0.9	3.3±0.5	3.4±2.6	0.17±0.03	0.17±0.13	0.23	0.79±0.05
H-PB3#3	20.0	2.1	3.2±0.2	14±4.6	0.16±0.01	0.68±0.24	0.24	0.74±0.05
D-PZ#1	3.0	1.8	7.0±0.2	6.8±1.3	2.33±0.05	2.27±0.43	1.08	2.4±0.05
H-PZ2#1	3.0	2.3	3.6±0.1	(-5.1±1.4)	1.20±0.02	(-1.70±0.47)	1.00	1.3±0.02
D-PZ3#1	3.0	1.9	6.4±0.2	6.2±1.4	2.13±0.05	2.07±0.47	1.08	2.2±0.05
H-PZ4#1	3.0	3.6	4.8±0.1	1.9±1.4	1.60±0.02	0.63±0.47	0.86	2.1±0.03
D-PZ5#1	3.0	2.0	7.1±0.2	1.3±1.4	2.38±0.03	0.42±0.45	1.04	2.5±0.03
H-PZ6#1	3.0	5.9	7.1±0.1	(-0.2±1.4)	2.36±0.02	(-0.08±0.48)	1.34	1.9±0.02
Average for PZ		(D)	6.9±0.4	4.8±3.0	2.3±0.1	1.6±1.0	1.1±0.0	2.4±0.2
		(H)	5.2±1.8	(-1.1±3.6)	1.7±0.6	(-0.4±1.2)	1.1±0.3	1.8±0.4